Biochemical and Biophysical Research Communications 424 (2012) 446–450

Contents lists available at SciVerse ScienceDirect

Biochemical and Biophysical Research Communications

journal homepage: www.elsevier.com/locate/ybbrc

Nanoelectroablation therapy for murine basal cell carcinoma

Richard Nuccitelli [a,*], Kevin Tran [a], Brian Athos [a], Mark Kreis [a], Pamela Nuccitelli [a], Kris S. Chang [b], Ervin H. Epstein Jr. [b], Jean Y. Tang [b,c]

[a] BioElectroMed Corp., 849 Mitten Rd., Suite 104, Burlingame, CA 94010, USA
[b] The Children's Hospital Oakland Research Institute, Oakland, CA 94609, USA
[c] Stanford University, Stanford, CA 94305, USA

ARTICLE INFO

Article history:
Received 18 June 2012
Available online 4 July 2012

Keywords:
Nanosecond pulsed electric fields
Basal cell carcinoma
Apoptosis
DNA fractionation
Pyknosis
Ablation
Nanoelectroablation

ABSTRACT

When skin tumors are exposed to non-thermal, low energy, nanosecond pulsed electric fields (nsPEF), apoptosis is initiated both *in vitro* and *in vivo*. This nanoelectroablation therapy has already been proven effective in treating subdermal murine allograft tumors. We wanted to determine if this therapy would be equally effective in the treatment of autochthonous BCC tumors in Ptch1$^{+/-}$K14-Cre-ER p53 fl/fl mice. These tumors are similar to human BCCs in histology [2,20] and in response to drug therapy [19]. We have treated 27 BCCs across 8 mice with either 300 pulses of 300 ns duration or 2700 pulses of 100 ns duration, all at 30 kV/cm and 5–7 pulses per second. Every nsPEF-treated BCC began to shrink within a day after treatment and their initial mean volume of 36 ± 5 (SEM) mm^3 shrunk by 76 ± 3% over the ensuing two weeks. After four weeks, they were 99.8% ablated if the size of the treatment electrode matched the tumor size. If the tumor was larger than the 4 mm wide electrode, multiple treatments were needed for complete ablation. Treated tumors were harvested for histological analysis at various times after treatment and exhibited apoptosis markers. Specifically, pyknosis of nuclei was evident as soon as 2 days after nsPEF treatment, and DNA fragmentation as detected via TUNEL staining was also evident post treatment. Nanoelectroablation is effective in triggering apoptosis and remission of radiation-induced BCCs with a single 6 min-long treatment of 2700 pulses.

1. Introduction

Basal cell carcinoma (BCC) is the most commonly occurring cancer in the United States [15], and the major known risk factor is exposure to solar UV radiation. Most BCCs are treated with surgical excision or electro-desiccation and curettage, both of which can be scarring [21]. Because BCC tumors are so common, especially in the elderly population, the cost and burden of BCC treatment has been estimated to be the 4th most costly cancer in the Medicare population [15]. Our goal is to find a novel, quick, less expensive and effective treatment for BCCs.

There are currently four non-thermal therapies being tested on various tumor types in clinical trials. These include: (1) Electrochemotherapy in which 100 μs long pulses are used to electroporate the plasma membrane to introduce impermeable chemotherapeutic drugs to tumors [6,9]; (2) Electro-gene therapy which uses electroporation to deliver genes that locally activate the immune system [8]; (3) Irreversible electroporation which uses higher voltage, 100 μs pulses to introduce irreversible pores in the plasma membrane to initiate necrosis [4]; and (4) Nanoelectroablation which uses nanosecond pulsed electric fields (nsPEF) to transiently form nanopores in both the plasma membrane and organelle membranes and trigger apoptosis [17]. The advantage of nanoelectroablation over the others is that it does not require the addition of any substances around the treated tumor and the slower apoptotic cell death allows time for possible activation of the immune response [12]. One disadvantage is that the electrode must encapsulate the entire tumor in order to ablate it with a single treatment.

We have previously shown that nanoelectroablation therapy ablates melanoma tumors in murine allografts [3,10,11,13]. The anti-tumor effect of these ultra-short, high voltage pulses is due to the generation of transient nanopores in both the plasma and intracellular membranes in treated tumor cells [16]. These nanopores allow transmembrane movement of small molecules and ions, leading to the elevation of intracellular Ca^{2+} and triggering apoptosis [1,14,16] and tumor ablation.

Here we describe our studies of nanoelectroablation of murine BCCs developing in the skin as a result of radiation exposure as pups. These BCCs are much more similar to those found in humans

Abbreviations: kV, kilovolts; UV, ultraviolet; BCC, basal cell carcinoma; nsPEF, nanosecond pulsed electric field; ns, nanosecond; m, meter; cm, centimeter; min, minutes; SEM, standard error of the mean; TUNEL, terminal deoxynucleotidyl transferase dUTP nick end labeling.

* Corresponding author. Fax: +1 650 697 3737.
E-mail address: rich@bioelectromed.com (R. Nuccitelli).

0006-291X/$ - see front matter © 2012 Elsevier Inc. All rights reserved.
http://dx.doi.org/10.1016/j.bbrc.2012.06.129

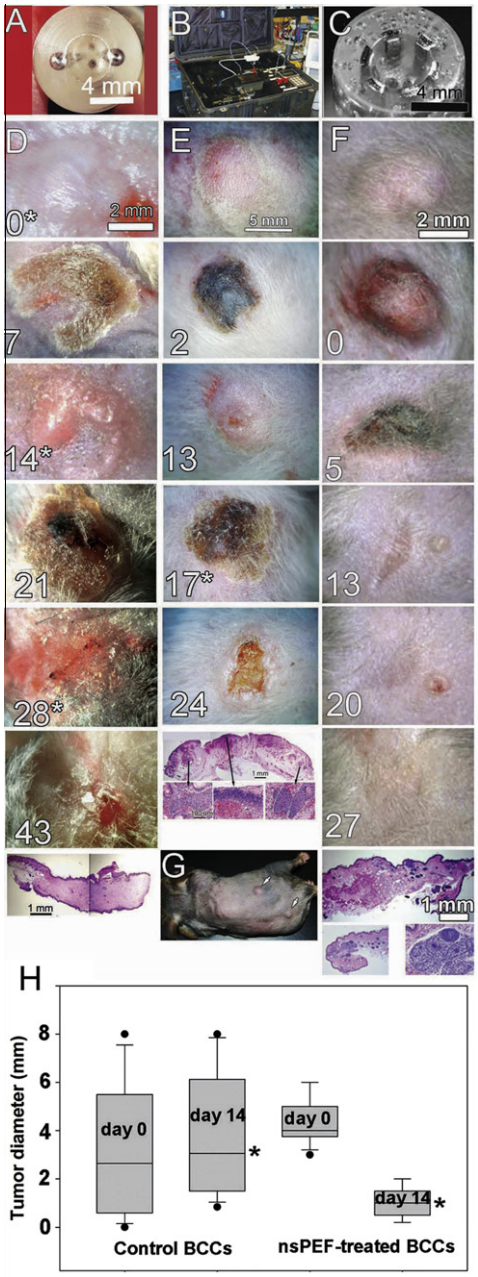

Fig. 1. Three most common outcomes from BCC nanoelectroablation therapy. (A) 2-Post suction electrode used in "D"; (B) PulseCure® Model S-3 pulse generator; (C) 6-Post suction electrode used in "E" and "F". (D) **Outcome 1:** Complete tumor ablation following multiple treatments. 4 mm-wide BCC that was treated with 300 pulses from the 2-post electrode on days marked with asterisk. Images below it were taken on the day after treatment indicated. (E) **Outcome 2:** Incomplete tumor ablation when treatment electrode was smaller than tumor. A 7.4 mm-wide BCC was treated with a 4 mm-wide dual post electrode (1C) with photos below taken on the day indicated. 2700 pulses were applied at 7 Hz on day 0 and day 17. (F) **Outcome 3:** Nearly complete ablation results when the treatment electrode size matches the tumor size. 4 mm-wide BCC before treatment with 6-post electrode connected so that two neighboring electrodes were at one polarity and the opposing pair was at the opposite polarity applying 2000 pulses of 30 kV/cm at 5 pulses per second. Photos after treatment are shown in the column below taken on the days indicated. The H&E stained sections at the bottom of each column were prepared on the same day as the last photograph shown. The magnifications of the lower two images in the right column are 2.5 and 10 times greater, respectively, than the one with the scale bar. A few small remnants of BCC are still present in these sections. (G) Photo of a mouse with 2 BCCs (arrows) prior to treatment; (H) Box plot of the diameters of 8 control BCCs and 15 nsPEF-treated BCCs measured over a 14-day period measured. *There is a significant difference between the median 14-day tumor sizes ($p = 0.002$).

and therefore are a more relevant model system to demonstrate the efficacy of nanoelectroablation.

2. Methods

2.1. NsPEF pulse generators

Three different pulse generators were used in this study and all of them generated a square wave with a rise time of 15–25 ns. Model S-1 was a 300 ns pulse generator using a single Blumlein line composed of a 60 m long coaxial cable. The load and matching resistor were placed at the center of the cable and the two 30 m long halves were wound around a cylinder. When the combination of load and matching impedance is equal to two times the 50 Ω cable impedance, the full amplitude is delivered with little or no reflection. With a typical load impedance of approximately 750 Ω, we added a matching resistor of 115 Ω in parallel to the load to balance the total impedance to 100 Ω. The second pulse generator (Model S-2) used the same design as S-1 with a 20 m long coaxial cable to generate a 100 ns long pulse. The two 10 m long halves fit within cardboard cylinders. The third design (Model S-3, Fig. 1B) placed two Blumlein lines in series (also known as a double-Blumlein pulse forming network). The advantage of this advanced design is that the system need only be charged to half of the desired delivery pulse amplitude. These were 50 Ω RG-174/U coaxial cables, each of them 20 m long, wound on a cardboard cylinder. When the load impedance is equal to four times that of the coaxial cable, the full amplitude is delivered with little to no reflection. Since our load impedance was typically 750 Ω, we used a 270 Ω matching resistor in parallel with the load to balance the load to 200 Ω. When discharged through a triggered spark gap at atmospheric pressure, this arrangement delivers a 100 ns-long pulse with a 20 ns rise time. We used a microprocessor to trigger the spark gap at either 5 or 7 Hz, control the voltage level of the power supply, and count the pulses. The pulse counter utilized the signal generated by a custom current sensor placed around one of the wires connected to the suction electrode so that only pulses resulting in current delivery to the tumor were counted.

2.2. Delivery electrodes

We used three suction electrode configurations (Fig. 1A, C), two of which used the same physical electrode (Fig. 1C) with different electrical connections. In the 6-post singular configuration, one of the 6 posts was positive and the post directly across from it was negative. In the 6-post dual configuration, two neighboring posts were positive and the pair directly across from them was negative. This dual configuration generated the most uniform electric field between the electrodes and also gave the best ablation of BCCs. The electrodes employ a suction feature to hold the soft, pliable skin of the mice within the cavity between electrodes. During pulse application, the treatment was paused after each group of 500 pulses and we rotated the electrode 90° to provide a uniform coverage over the entire tumor.

2.3. Mice

Ptch1$^{+/-}$K14-Cre-ER p53 fl/fl mice [7] were used for these studies. They were exposed to a 5 Gy dose of ionizing radiation (Cs-137) weekly between 2 months and 12 months of age to induce several BCCs on their backs. This work was carried out over a period of two years as tumors appeared on the mice several months after exposure to radiation. All the treatments had to be done in the animal facility at The Children's Hospital Oakland Research

Table 1
Summary of BCC nanoelectroablation treatments.

Mouse	Tumor No.	Diam. (mm)	1st treat[a]	2nd treat	3rd treat	Electrode type	Days post treat biopsy
3597	8	5	3/21/08			4 mm para. plate, 300 ns	4
3645	1	5	3/21/08			4 mm para. plate 300 ns	4
3597	4	5	3/21/08			4 mm para. plate 300 ns	17
3597	1	5	3/21/08			4 mm para. plate, 300 ns	26
3597	5	5	3/21/08			4 mm para. plate, 300 ns	39
3597	11–12	5	4/29/08			4 mm-2 post, 300 ns	36
3597	13	5	4/29/08			4 mm-2 post, 300 ns	36
3752	1	4	9/24/08	10/08/08	10/22/08	4 mm-2 post, 300 ns	43
5033	1	7.4	1/14/09	1/20/09	1/28/05	Needle, 100 ns	44
5033	2	4	1/14/09	1/20/09	2/3/09	6-postsing, 100 ns	44
5033	5	4	2/3/09	2/16/09		6-postsing, 100 ns, 10 hz	24
5033	6	4	2/3/09	2/16/09		6-postdual, 100 ns, 7 hz	24
5033	7	5	2/16/09			6-postdual, 100 ns, 7 hz	11
5033	8	5	2/16/09			6-postsing, 100 ns, 7 hz	11
5040	1	4.5	1/14/09			6-post sing, 100 ns	6
5040	2	3	1/20/09	1/28/09		Needle, 1776p; 769 p	16
5040	3	4	2/3/09			6-postdual, 100 ns	2
5040	4	10	1/28/09			Needle, 2705 p, 100 ns	8
5041	2	6	1/26/09	2/13/09		6-postdual, 100 ns	Poor fix
5041	4	5	1/26/09	2/13/09		6-postsing, 100 ns	Poor fix
5042	2	4	1/26/09	2/13/09		6-postdual, 100 ns	39
5042	4	4	1/26/09	2/13/09		6-postsing, 100 ns	39
5034	1	6	2/3/09	2/16/09		6-postsing, 100 ns	24
5034	3	8	2/3/09	2/20/09		8 mm needle, 100 ns	24
5034	4	5	2/20/09			4 mm needle, 100 ns	7
5034	5	4	2/20/09			4 mmneedle, 100 ns	7
5755	4	3.5	12/8/09			6-post dual, 100 ns	15
5756	1	3.5	1/6/10			6-post dual, 100 ns	27
5756	2	4	1/6/10			6-post dual, 100 ns	27
5756	3	3	1/11/10			6-post dual, 100 ns	13
5756	4	3	1/19/10			6-post dual, 100 ns	13
5756	5	3	1/19/10			6-post dual, 100 ns	5
5756	6	3	1/19/10			6-post dual, 100 ns	5

[a] Tumors 2, 3, 6, 7, 9, 19 on mouse 3597 were untreated controls.

Institute (CHORI) so we transported the pulser there for each treatment. When the work began we did not know the optimal electrode configuration so we used five different ones as described below.

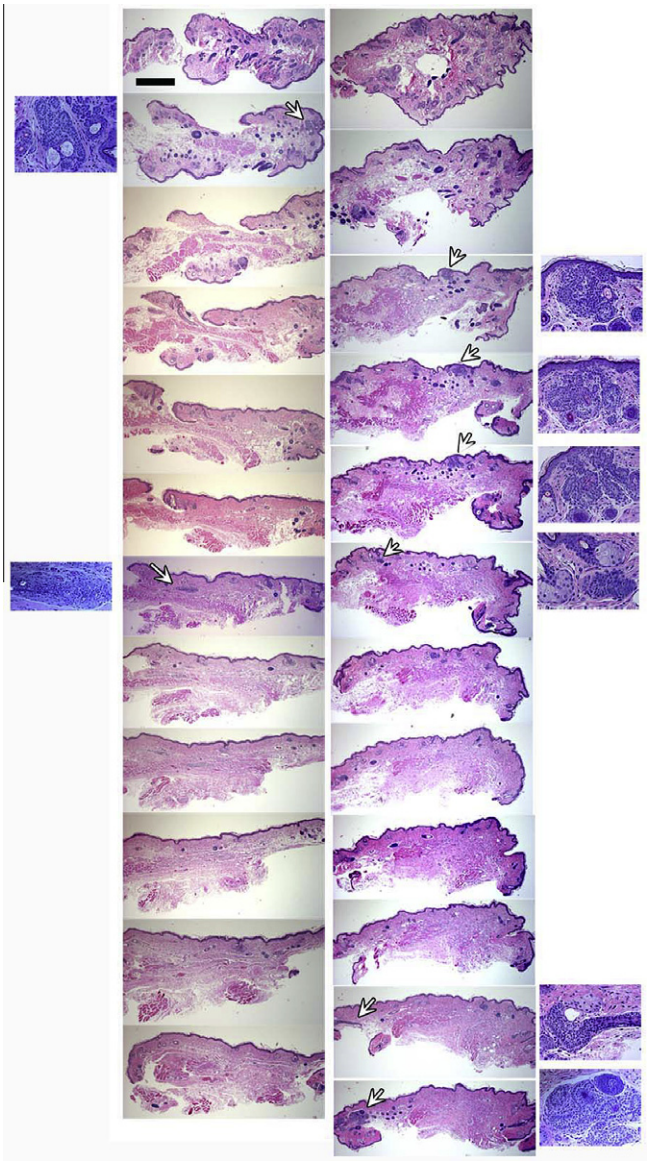

Fig. 2. Serial sections from an ablated BCC taken at 50 μm intervals 27 days after treatment using a 6-post dual configuration electrode. Scale bar in upper left indicates 1 mm and applies to both columns of sections. A 10× magnified view of small remnants of BCC are shown next to some sections with an arrow indicating their location in the section.

3. Results

Autochthonous BCC tumors in Ptch1$^{+/-}$K14-Cre-ER p53 fl/fl mice are similar to human BCCs in histology [2,20] and in response to drug therapy [19]. We treated 27 BCCs (n = 8 mice) with suction electrodes (Fig. 1B), delivering 300–2700 pulses, 30 kV/cm in amplitude, 100 ns long, at a pulse rate of 5–7 pulses per second as summarized in Table 1. We kept track of tumor locations with tattoo marks on opposite sides of the tumors and frequent photographs. BCCs began to show epidermal necrosis within two days, and all nsPEF-treated BCCs responded with clinical regression. Their initial mean volume of 36 ± 5 (SEM) mm^3 (4.1 mm diameter) shrunk by 76 ± 3% over the ensuing two weeks (Fig. 1D–H), whereas 8 untreated control tumors on our untreated vehicle group increased in size by 17% over the same period. Within four weeks after nanoelectroablation, most treated tumors exhibited nearly complete regression depending on two treatment parame-

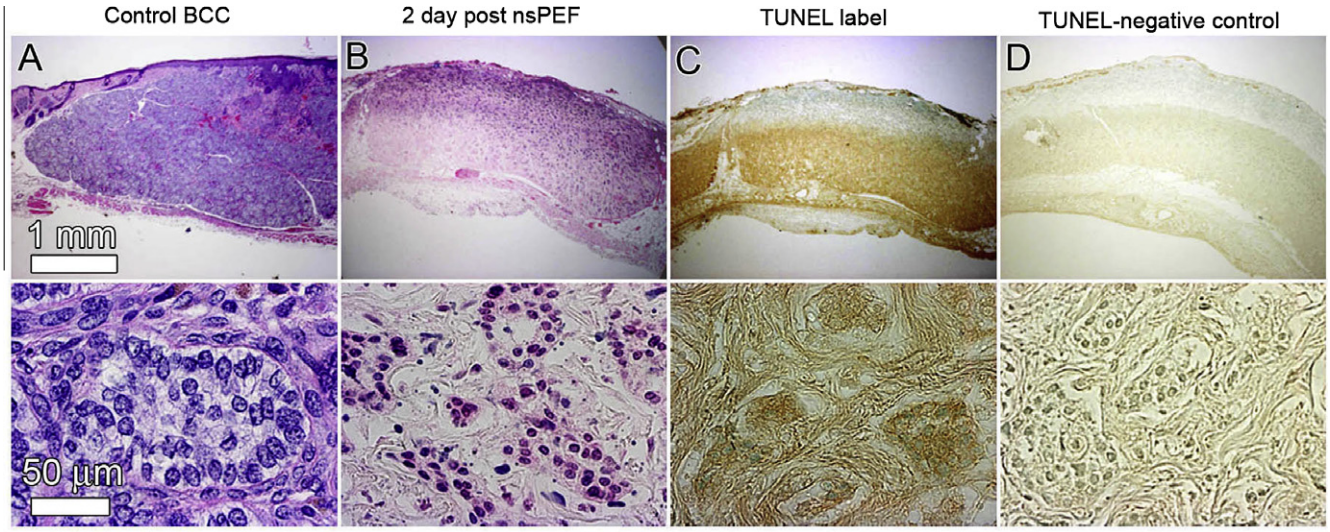

Fig. 3. BCC fixed 2 days after nsPEF treatment exhibits pyknosis and DNA fragmentation. Top and bottom rows are the same image at different magnifications indicated by scale bars on far left. (A) Control BCC for comparison at two magnifications; (B) BCC was treated with 2700 pulses 100 ns, 30 kV/cm, two days before excision, fixation, sectioning and labeling with H&E. Pyknosis is evident in nuclei; (C) TUNEL staining (Brown) that indicates fragmented DNA; (D) Negative control for TUNEL staining.

ters: (1) electrode configuration and (2) complete encapsulation of targeted tumor with the electrode. The best results were obtained using the 6-post electrode (Fig. 1C), in the dual configuration. Of the 10 tumors treated with this electrode, only one that was 4 mm or less in diameter required a second treatment in order to ablate it (Table 1). In contrast, 7 of the 10 tumors treated with the 2-post electrode required additional treatments to ablate (Fig. 1D). Electrode size was also critical. If the BCC was larger than the electrode, only partial ablation was obtained even with multiple treatments (Fig. 1E). Ten of the 27 treated tumors fell into this category. These additional treatments were applied in two-week intervals. Only three tumors were treated 3 times and one is shown in Fig. 1D.

In order to confirm ablation we performed serial section histology on two tumors selected from the 4 single-treatment tumors that fit precisely within the 6-post electrode. Through 3D reconstructions of the serial sections (Fig. 2), we observed only microscopic, residual BCCs whose total volume was only 0.2% of the original tumor volume. It remains to be seen whether these small residual BCCs would lead to recurrence because these animals continuously develop BCCs and do not live very long. However, when a similar nsPEF treatment was applied to murine melanomas in an allograft system, the tumors did not recur over a 4-month observation period following ablation [10].

Consistent with the reported induction of apoptosis by nanoelectroablation in cultured tumor cells *in vitro* [5,18], we observed pyknosis (Fig. 3B) and DNA fragmentation by TUNEL labeling of treated tumors (Fig. 3C) 2 days following nsPEF treatment.

4. Discussion

4.1. Main findings

We have found that endogenous BCC tumors growing naturally in mouse skin can be ablated using the same pulse parameters found to ablate tumors developing from subdermally-injected tumor cells in the murine allograft model system. From these studies and others we learned that electrodes using the 6-pole dual configuration exhibited the most complete tumor ablation, particularly when the electrode completely surrounded the tumor. We also observed pyknosis and DNA fragmentation in the treated tumors, both indicators of apoptosis.

4.2. Advantages and disadvantages of nanoelectroablation

The main advantage of this technique is that it is non-thermal and does not require the addition of any chemicals to ablate. In addition, the relatively slow ablation time of about 4 weeks allows the immune system to be sensitized to the tumor cells and inhibit the growth of secondary tumors following metastasis [12]. The main disadvantage is the high voltage required to generate the effective field strength of 30 kV/cm that is required to obtain an effective ablation [11]. This high field requirement is challenging due to the ionization of gases and subsequent spark generation at those high voltages. All metal surfaces on the electrode must be coated with a dielectric such as olive oil to prevent gas exposure to those surfaces. We used an electrode spacing of 5 mm so that we only needed to apply a voltage difference of 15 kV to obtain the required 30 kV/cm. This 5 mm treatment region means that larger tumors have to be treated multiple times in different locations in order to ablate the entire tumor.

The microscopic remnants of BCCs that we observed in the serial sections suggest that nanoelectroablation does not completely ablate the tumor in mice. However, our preliminary results from treating human BCCs with nanoelectroablation show complete ablation without microscopic remnants in most instances. Nanoelectroablation offers a new therapy for the treatment of basal cell carcinomas and other skin lesions. It triggers apoptosis in all of the cells between the electrodes and causes very little scarring. We are now conducting a pilot clinical trial using nanoelectroablation therapy on human BCCs to determine the safety, tolerability, and efficacy for the primary treatment of BCCs or as an adjuvant to surgery (Clinicaltrials.gov ID: NCT01463709).

Acknowledgments

We thank Yefim Khaimisky for help raising these animals. BioElectroMed built the prototype PulseCure® Models used in these experiments but is not marketing these pulse generators. This work was supported by NIH Grants R43CA123924 and R01CA125722 to RN.

References

[1] F.M. Andre, M.A. Rassokhin, A.M. Bowman, A.G. Pakhomov, Gadolinium blocks membrane permeabilization induced by nanosecond electric pulses and reduces cell death, Bioelectrochemistry 79 (2010) 95–100.

[2] M. Aszterbaum, J. Epstein, A. Oro, V. Douglas, P.E. LeBoit, M.P. Scott, E.H. Epstein Jr., Ultraviolet and ionizing radiation enhance the growth of BCCs and trichoblastomas in patched heterozygous knockout mice, Nat. Med. 5 (1999) 1285–1291.

[3] X. Chen, R.J. Swanson, J.F. Kolb, R. Nuccitelli, K.H. Schoenbach, Histopathology of normal skin and melanomas after nanosecond pulsed electric field treatment, Melanoma Res. 19 (2009) 361–371.

[4] R.V. Davalos, I.L. Mir, B. Rubinsky, Tissue ablation with irreversible electroporation, Ann. Biomed. Eng. 33 (2005) 223–231.

[5] W.E. Ford, W. Ren, P.F. Blackmore, K.H. Schoenbach, S.J. Beebe, Nanosecond pulsed electric fields stimulate apoptosis without release of pro-apoptotic factors from mitochondria in B16f10 melanoma, Arch. Biochem. Biophys. 497 (2010) 82–89.

[6] J. Gehl, Electroporation for drug and gene delivery in the clinic: doctors go electric, Methods Mol. Biol. 423 (2008) 351–359.

[7] L.V. Goodrich, L. Milenkovic, K.M. Higgins, M.P. Scott, Altered neural cell fates and medulloblastoma in mouse patched mutants, Science 277 (1997) 1109–1113.

[8] L.C. Heller, R. Heller, In vivo electroporation for gene therapy, Hum. Gene Ther. 17 (2006) 890–897.

[9] L.M. Mir, N. Morsli, J.R. Garbay, V. Billard, C. Robert, M. Marty, Electrochemotherapy: a new treatment of solid tumors, J. Exp. Clin. Cancer Res. 22 (2003) 145–148.

[10] R. Nuccitelli, X. Chen, A.G. Pakhomov, W.H. Baldwin, S. Sheikh, J.L. Pomicter, W. Ren, C. Osgood, R.J. Swanson, J.F. Kolb, S.J. Beebe, K.H. Schoenbach, A new pulsed electric field therapy for melanoma disrupts the tumor's blood supply and causes complete remission without recurrence, Int. J. Cancer 125 (2009) 438–445.

[11] R. Nuccitelli, U. Pliquett, X. Chen, W. Ford, S.R. James, S.J. Beebe, J.F. Kolb, K.H. Schoenbach, Nanosecond pulsed electric fields cause melanomas to self-destruct, Biochem. Biophys. Res. Commun. 343 (2006) 351–360.

[12] R. Nuccitelli, K. Tran, K. Lui, J. Huynh, B. Athos, M. Kress, P. Nuccitelli, E.C. De Fabo, Non-thermal nanoelectroablation of UV-induced murine melanomas stimulates an immune response. Pigment Cell Melanoma Res. in press.

[13] R. Nuccitelli, K. Tran, S. Sheikh, B. Athos, M. Kreis, P. Nuccitelli, Optimized nanosecond pulsed electric field therapy can cause murine malignant melanomas to self-destruct with a single treatment, Int. J. Cancer 127 (2010) 1727–1736.

[14] A.G. Pakhomov, A.M. Bowman, B.L. Ibey, F.M. Andre, O.N. Pakhomova, K.H. Schoenbach, Lipid nanopores can form a stable, ion channel-like conduction pathway in cell membrane, Biochem. Biophys. Res. Commun. 385 (2009) 181–186.

[15] H.W. Rogers, M.A. Weinstock, A.R. Harris, M.R. Hinckley, S.R. Feldman, A.B. Fleischer, B.M. Coldiron, Incidence estimate of nonmelanoma skin cancer in the United States, Arch. Dermatol. 146 (2010) 283–287.

[16] K.H. Schoenbach, Bioelectric effect of intense nanosecond pulses, in: A.G. Pakhomov, D. Miklavcic, M.S. Markov (Eds.), Advanced Electroporation Techniques in Biology and Medicine, Taylor and Francis Group, Boca Raton, 2010, pp. 19–50.

[17] K.H. Schoenbach, R.P. Joshi, J.F. Kolb, N. Chen, M. Stacey, E.S. Buescher, S.J. Beebe, P. Blackmon, Ultrashort electrical pulses open a new gateway into biological cells, Proc. IEEE 92 (2004) 1122–1137.

[18] K.H. Schoenbach, R. Nuccitelli, S.J. Beebe, Zap, Spectrum IEEE 43 (2006) 20–26.

[19] J.Y. Tang, M. Aszterbaum, M. Athar, F. Barsanti, C. Cappola, N. Estevez, J. Hebert, J. Hwang, Y. Khaimskiy, A. Kim, Y. Lu, P.L. So, X. Tang, M.A. Kohn, C.E. McCulloch, L. Kopelovich, D.R. Bickers, E.H. Epstein Jr., Basal cell carcinoma chemoprevention with nonsteroidal anti-inflammatory drugs in genetically predisposed PTCH1+/− humans and mice, Cancer Prev. Res. (Phila) 3 (2010) 25–34.

[20] G.Y. Wang, J. Wang, M.L. Mancianti, E.H. Epstein Jr., Basal cell carcinomas arise from hair follicle stem cells in Ptch1(+/−) mice, Cancer Cell. 19 (2011) 114–124.

[21] T. Wetzig, M. Woitek, K. Eichhorn, J.C. Simon, U. Paasch, Surgical excision of basal cell carcinoma with complete margin control: outcome at 5-year follow-up, Dermatology 220 (2010) 363–369.